

1 **Exploring the effect of sex on an empirical fitness landscape**

2 J. Arjan G. M. de Visser^{1,*}, Su-Chan Park^{2,†}, and Joachim Krug^{2,‡}

3 1. Laboratory of Genetics, Wageningen University, Arboretumlaan 4, 6703BD Wageningen,
4 The Netherlands; 2. Institute for Theoretical Physics, University of Cologne, Zùlpicher Str.
5 77, 50937 Cologne, Germany

6 Received _____; accepted _____

Prepared as article for the American Naturalist.

Contains appendices A and B, 3 tables and 7 figures (figures 2-7 are color figures)

*Corresponding author; e-mail: Arjan.devisser@wur.nl

†E-mail: psc@thp.uni-koeln.de

‡E-mail: krug@thp.uni-koeln.de

ABSTRACT

The nature of epistasis has important consequences for the evolutionary significance of sex and recombination. Recent efforts to find negative epistasis as source of negative linkage disequilibrium and associated long-term sex advantage have yielded little support. Sign epistasis, where the sign of the fitness effects of alleles varies across genetic backgrounds, is responsible for ruggedness of the fitness landscape with implications for the evolution of sex that have been largely unexplored. Here, we describe fitness landscapes for two sets of strains of the asexual fungus *Aspergillus niger* involving all combinations of five mutations. We find that $\sim 30\%$ of the single-mutation fitness effects are positive despite their negative effect in the wild-type strain, and that several local fitness maxima and minima are present. We then compare adaptation of sexual and asexual populations on these empirical fitness landscapes using simulations. The results show a general disadvantage of sex on these rugged landscapes, caused by the break down by recombination of genotypes escaping from local peaks. Sex facilitates escape from a local peak only for some parameter values on one landscape, indicating its dependence on the landscape's topography. We discuss possible reasons for the discrepancy between our results and the reports of faster adaptation of sexual populations.

Keywords: evolution of sex, sign epistasis, fitness landscape, recombination

1. Introduction

11 The way genes interact in their effect on a phenotype or fitness, called epistasis,
12 has important implications for evolution, including the evolution of sex and recombina-
13 tion (Wolf et al. 2000). Epistasis entails any deviation from independent (i.e. additive
14 or multiplicative, depending on the evolutionary model used) gene effects, and hence
15 encompasses many different forms of gene interaction. At least two forms of epistasis
16 are relevant for the question why sex and recombination have evolved. The first is a
17 one-dimensional type of magnitude epistasis, called *negative epistasis*, where the fitness
18 effects of alleles all have the same sign (i.e. all are either deleterious or beneficial) and the
19 fitness of genotypes with many alleles is lower than expected from the product of their
20 individual effects (Barton 1995; Otto and Lenormand 2002). Negative epistasis provides a
21 long-term advantage to sex and recombination by causing negative linkage disequilibria of
22 alleles affecting fitness (Barton 1995). By breaking down linkage disequilibria and increasing
23 fitness variation, sex may facilitate the response to selection due to the net production of
24 genotypes carrying extreme numbers of fitness alleles. Besides negative epistasis, genetic
25 drift combined with directional selection can cause negative linkage disequilibria (Barton
26 1995; de Visser and Elena 2007; Kondrashov 1993; Otto and Lenormand 2002). However,
27 magnitude epistasis also has consequences for fitness in the next generation, and it is
28 the balance between short- and long-term effects of sex that determines the conditions
29 favoring selection for sex and recombination (Barton 1995; Otto and Lenormand 2002).
30 Most experimental studies have concentrated on detecting magnitude epistasis, but
31 despite increasing efforts during the last decade the support for negative epistasis is
32 limited (de Visser and Elena 2007; Kouyos et al. 2007).

33 The second type of epistasis with potential implications for the evolution of sex
34 is *sign epistasis*, where the sign of the fitness effects of alleles varies across genetic

35 backgrounds (Weinreich et al. 2005). Sign epistasis causes adaptive constraints by limiting
36 the number of mutational pathways that can be taken by natural selection. If sign epistasis
37 is locally consistent, such that all mutational pathways leading to a particular genotype
38 show the same fitness change upon approach of that genotype, these constraints are most
39 severe and cause local fitness peaks and valleys (Weinreich et al. 2005).

40 The effect of sex on rugged fitness landscapes has received little attention, but
41 is likely to depend on the landscape’s topography, and thus is largely an empirical
42 problem. Unlike tests of negative epistasis, which are possible with phenotypic analyses
43 (see Kouyos et al. (2007)), conclusive tests of sign epistasis require knowledge of the
44 genotypes involved. Moreover, to study evolutionary constraints from sign epistasis,
45 a systematic and detailed description of the fitness landscape is needed, requiring the
46 construction and fitness measurement of many genotypes. These requirements clearly
47 constrain empirical studies of fitness landscapes. However, with the advent of genomic
48 techniques recent studies have begun to tackle this problem, which found ample support for
49 sign epistasis (Weinreich et al. 2006; Weinreich et al. 2005; Poelwijk et al. 2007; Salverda
50 et al. unpublished). Indirect support for fitness landscapes with multiple peaks has come
51 from the analyses of fitness trajectories of evolution experiments with micro-organisms,
52 where replicate populations sometimes approach different fitness maxima (Buckling et al.
53 2003; Burch and Chao 2000; Korona et al. 1994; Rozen et al. 2008; Schoustra et al. 2007).
54 Outside the realm of evolutionary computation (Watson and Wakeley 2006), theoretical
55 studies of the effect of sex on rugged fitness landscapes are rare. One study, which
56 modeled a specific landscape with a single narrow ridge of increasing fitness, found
57 that sex slows down adaptation (Kondrashov and Kondrashov 2001), while a study that
58 modified this model to include isolated peaks occupied by a polymorphic population found
59 a sex benefit (Watson and Wakeley 2006). Finally, a study using a multi-locus rugged
60 fitness landscape generated according to Kauffman’s NK-model (Kauffman 1993) found

61 faster adaptation due to recombination for the parameter values used, particularly when
62 recombination rates were negatively associated with fitness (Hadany and Beker 2003).

63 The aim of the present paper is twofold. We first analyze fitness data of the filamentous
64 fungus *Aspergillus niger* in order to detect and quantify the occurrence of sign epistasis
65 and multiple fitness peaks, and then explore the effects of sex on these empirical landscapes
66 using simulations. The data involve two collections of strains that each carry all possible
67 combinations of five phenotypic marker mutations with individually deleterious effect
68 (four of which are shared by the two collections). These data were collected and analyzed
69 previously to test for prevailing negative epistasis among deleterious mutations, for which we
70 found no significant support (de Visser et al. 1997). Our new analyses indicate the presence
71 of sign epistasis: we find both negative and positive fitness changes by the addition of single
72 mutations depending on the genetic background. We also find local fitness maxima and
73 minima in both data sets, leading to severe adaptive constraints. We then use simulations
74 to compare adaptation of sexual and asexual populations on these empirical rugged fitness
75 landscapes. We find that populations always get stuck on local peaks, from which they may
76 later escape via the production of genotypes containing multiple mutations. The simulation
77 results suggest that sex is disadvantageous under most conditions by breaking down escape
78 genotypes. Only on one landscape and for intermediate recombination rates, sex facilitates
79 the escape from a local to the global peak, hence indicating that this benefit depends on
80 the landscape’s topography. We discuss these findings in the light of experimental evidence
81 for sex benefits during adaptation.

2. Methods

2.1. Strain construction

Aspergillus niger is an asexual filamentous fungus with a predominantly haploid life cycle. A detailed description of the construction of the *A. niger* strains used in this study is given in (de Visser et al. 1997). Briefly, haploid segregants were isolated from a diploid between a wild-type strain and a strain containing a single marker mutation on each of its eight chromosomes. Both the wild-type and the eight-marker strain contained a spore-color marker on its first chromosome (*olvA1* and *fwnA1*, causing olive- and fawn-colored conidiospores, respectively), which was helpful for the isolation of haploid segregants from the diploid mycelium which produced black spores. The seven marker mutations on the other chromosomes include, in increasing chromosomal order: *argH12* (arginine deficiency), *pyrA5* (pyrimidine deficiency), *leuA1* (leucine deficiency), *pheA1* (phenyl-alanine deficiency), *lysD25* (lysine deficiency), *oliC2* (oligomycin resistance), and *crnB12* (chlorate resistance). These marker mutations were arbitrarily chosen and the only requirement was their phenotypic detectability. They were individually introduced using low-dose UV induction, and combined using mitotic recombination to minimize the probability of introducing additional mutations. Because the wild-type and eight-marker strain had a recent common ancestor, it was unlikely that the segregants differed at more loci than those carrying the marker mutation.

From the $2^8 = 256$ theoretically possible different haploid segregants, 186 were isolated after forced haploidization on medium containing benomyl from among ~ 2500 strains tested. Among those strains, two sets of 32 strains each were present that carry all 32 possible combinations of five markers: the wild type (no mutations), the five strains with a single mutation, the 10 double mutants, the 10 triple mutants, the five quadruple mutants and the single quintuple mutant. One complete subset, referred to as CS I, involves all

107 combinations of *arg*⁻, *pyr*⁻, *leu*⁻, *oli*^R and *crn*^R; CS II contains all possible combinations
108 of *arg*⁻, *pyr*⁻, *leu*⁻, *phe*⁻ and *oli*^R. Hence, these two complete subsets share four of the
109 five marker mutations involved and are not independent. These complete subsets cover
110 all intermediates between wild-type and quintuple mutant, and thus allow a complete
111 description of the fitness landscape involved (Weinreich et al. 2006).

112 2.2. Fitness assay

113 Previously (de Visser et al. 1997), we used the increase in mycelial surface area per
114 unit time on supplemented medium as fitness estimate for these strains, because this
115 measure showed a strong positive correlation with the rate of spore production which is an
116 intuitive measure of fungal fitness (Pringle and Taylor 2002). There, we used deviations
117 from additivity at the level of log (surface area growth rate) as measure of epistasis. Here,
118 we use the rate of linear expansion of the radius of a colony spreading from a central source
119 to estimate fitness, because it is believed to be a better estimator of the intrinsic growth
120 rate (i.e. unhindered by competition), and because it is constant in time, which makes
121 departure from additive mutational effects a simple and appropriate way to detect epistasis.
122 However, radial growth rate and log (surface area growth rate) give almost identical results,
123 because using a linear model, variation in one fitness measure explains ~99.5% of the
124 variation in the other; the remaining ~0.5% is explained by the slight curvature of the
125 relationship. Moreover, many of our analyses require only a rank order of fitness values,
126 and hence are insensitive to these small differences.

127 The medium used for the fitness assay is a minimal agar medium supplemented with all
128 amino acids and nitrogen sources required by some of the auxotrophic strains (de Visser et al.
129 1997). The medium was prepared as a single batch and 9-cm petridishes were filled with
130 20mL medium using a calibrated pump. Two replicate plates were inoculated in the center

131 with spores from a pre-growth culture of each strain using a platinum needle. Plates were
 132 randomized and incubated at 26°C in the dark for 12 days. Colony diameter was measured
 133 after three and 12 days in two perpendicular directions, yielding a single estimate of the
 134 radial growth rate per replica plate by dividing the average difference in diameter in the two
 135 perpendicular directions at these two time points by twice (to derive radius from diameter)
 136 the time elapsed. All fitness estimates shown are expressed relative to that of the wild type.

137 2.3. Simulations

138 For the simulations of sexual and asexual populations, we use the Wright-Fisher model
 139 (Fisher 1930; Wright 1931) with a fixed number of haploid individuals N . The sequence
 140 length of genotypes (i.e. number of loci with two alleles each) is denoted by L which is 5
 141 for the *A. niger* landscapes, resulting in $2^5 = 32$ haploid genotypes. The algorithm to be
 142 employed for the recombination is similar to that described in (Kim and Orr 2005).

143 Let the frequency of the genotype σ at generation t be denoted by $f(\sigma; t)$. At first, the
 144 population evolves deterministically in the order of selection, mutation, and recombination.
 145 By selection and mutation, the frequency of the genotype σ at next generation will be

$$p_1(\sigma) = \sum_{\sigma'} \mu_{\sigma\sigma'} \frac{w(\sigma')}{\bar{w}(t)} f(\sigma'; t), \quad (1)$$

146 where $\bar{w}(t) \equiv \sum_{\sigma} f(\sigma; t)w(\sigma)$ is the mean fitness of the population at generation t and
 147 $\mu_{\sigma\sigma'}$ is the probability that the genotype σ' will be the genotype σ after mutation (if no
 148 mutation occurs, $\sigma = \sigma'$). In what follows, we use a mutation scheme such that

$$\mu_{\sigma\sigma'} = (1 - U) \delta_{\sigma\sigma'} + Z_{\sigma\sigma'} \frac{U}{L}, \quad (2)$$

149 where $\delta_{\sigma\sigma'}$ is the Kronecker delta which takes the value 1 if $\sigma = \sigma'$ and 0 otherwise, and

150 $Z_{\sigma\sigma'}$ is 1 if the Hamming distance between σ and σ' is 1 and 0 otherwise. This mutation
 151 scheme implies that a genotype can mutate with probability U and each change occurs only
 152 at one locus which is chosen at random on the sequence.

153 For the recombination scheme, we introduce $W_{\sigma|\sigma'\sigma''}$ which is the conditional probability
 154 that the resulting sequence is σ in case two sequences σ' and σ'' recombine. Although we
 155 studied three different recombination schemes (free recombination, one site exchange, and
 156 single crossover), we will only present the results for free recombination in what follows,
 157 because the conclusions for other recombination schemes are similar. Different forms of
 158 $W_{\sigma|\sigma'\sigma''}$ for other recombination schemes can be found in Appendix A.

159 By free recombination is meant that the new genotype is formed by the random choice
 160 of one of the alleles at each locus of two genotypes. For example, the possible recombinants
 161 of two sequences 11101 and 10100 by free recombination (with probability r) are 10100,
 162 10101, 11100, and 11101, each of which has equal probability to contribute to the frequency
 163 $p(\sigma)$ in equation (4). The free recombination probability can be written as

$$W_{\sigma|\sigma'\sigma''} = (1 - \delta_{\sigma'\sigma''}) \left[(\delta_{\sigma\sigma'} + \delta_{\sigma\sigma''}) \frac{1-r}{2} + \frac{r}{2^{d(\sigma',\sigma'')}} + (1 - \delta_{\sigma\sigma'}) (1 - \delta_{\sigma\sigma''}) F_{\sigma|\sigma'\sigma''} \frac{r}{2^{d(\sigma',\sigma'')}} \right] + \delta_{\sigma\sigma'} \delta_{\sigma\sigma''}, \quad (3)$$

164 where $d(\sigma', \sigma'')$ is the Hamming distance between two sequences in the argument and
 165 $F_{\sigma|\sigma'\sigma''}$ is 1 if σ can be a recombinant of σ' and σ'' and 0 otherwise.

166 Then the frequency of each genotype, after selection, mutation, and recombination,
 167 becomes

$$p(\sigma) = \sum_{\sigma', \sigma''} W_{\sigma|\sigma'\sigma''} p_1(\sigma') p_1(\sigma'') = p_1(\sigma)^2 + 2 \sum_{\langle \sigma', \sigma'' \rangle} W_{\sigma|\sigma'\sigma''} p_1(\sigma') p_1(\sigma''), \quad (4)$$

168 where $\langle \sigma', \sigma'' \rangle$ signifies that the sum runs over all pairs of distinct haploid genotypes. The

169 actual population at generation $t + 1$ is now formed by sampling N individual according to
170 the multinomial distribution with probability $p(\sigma)$.

171

3. Results

172

3.1. No prevailing magnitude epistasis

173

Figure 1 shows the relationship between relative fitness and mutation number for both
174 complete subsets of *A. niger* strains. Using surface area growth rate as measure of fitness
175 and regressing log fitness against mutation number, we (de Visser et al. 1997) previously
176 found no evidence for prevailing magnitude epistasis, because adding a quadratic term
177 to the linear regression model did not significantly improve the fit. Using radial growth
178 rate (RGR) to test for departure from additivity by regressing RGR against mutation
179 number confirms this conclusion. For both complete subsets of 32 strains, a linear model
180 explains most of the variation in RGR ($r^2 = 0.991$ and 0.992 , and the linear coefficient
181 $\alpha = -0.0816$ and -0.0773 for CS I and CS II, respectively; see fig. 1a and 1b). In fact, a
182 linear model explains more variation of the present fitness measure than it did for log fitness
183 in our previous analyses (for which we found $r^2 = 0.888$ and 0.881 , for CS I and CS II,
184 respectively), confirming that RGR is likely a more sensitive measure for detecting epistasis
185 as a departure from additivity. As before, a quadratic term, when added to the model, is
186 estimated to be positive ($\beta = 0.0102$ and 0.0069 for CS I and CS II, respectively), indicating
187 positive epistasis, but only approaches significance for CS I ($F_{1,30} = 4.135$, $P = 0.0509$)
188 and not for CS II ($F_{1,30} = 1.850$, $P = 0.184$). Hence, this analysis fails to reveal significant
189 magnitude epistasis in both data sets.

3.2. Mutational pathways reveal sign epistasis

190
191 Our previous analyses comparing the fitness of double mutants with the average of
192 both single mutants revealed the presence of both negative and positive epistasis, with the
193 majority of combinations showing positive epistasis (de Visser et al. 1997); this is probably
194 a consequence of the relatively large drop in fitness due to the first mutation, compared
195 to the overall linear trend in figure 1. We only determined whether the fitness of double
196 mutants was higher (indicating positive epistasis) or lower (indicating negative epistasis)
197 than expected from the fitness of both single mutants, and did not look for sign epistasis.
198 Here, we seek to reanalyze both complete subsets of 32 *A. niger* strains in order to detect
199 sign epistasis. To do so, we first analyze the $5! = 120$ possible pathways of five mutations
200 connecting wild-type and quintuple mutant to see whether the addition of some mutations
201 causes fitness to increase rather than decrease. Figure 1c and 1d shows these mutational
202 pathways for both complete subsets. Almost 80% of the 120 pathways exhibit one or more
203 mutational steps causing fitness to increase (95 in CS I and 93 in CS II). Since all mutations
204 are individually deleterious in the background of the wild-type strain, these fitness reversals
205 indicate sign epistasis among the mutations involved.

206 To formally demonstrate sign epistasis, we need to show the statistical significance of
207 the observed fitness reversals. Each complete subset contains 80 unique single-mutation
208 steps, and both subsets combined have 128 unique single-mutation steps (not 160, because
209 four of the five mutations are shared). Using conventional Bonferroni correction with a
210 cutoff P -value of 0.05 for all 128 tests combined renders none of the fitness differences
211 significant. Linear regression and ANOVA, however, show that genetic differences between
212 these strains are highly significant when tested collectively against the measurement error,
213 and explain almost 95% of the fitness variation within each complete subset de Visser et al.
214 (1997). The lack of significance of individual tests is therefore due to low statistical power

215 and not to a real absence of fitness differences, and is in part caused by the fact that only
216 two replicate fitness assays were performed (given that both subsets were part of a much
217 greater collection of strains that were assayed). A possible solution is to use a P -value of
218 0.05 for each individual test and accept that this leads to about six false positives in both
219 data sets combined (i.e. 128×0.05). Using this criterion, we find 40 single-mutation steps
220 with a significant fitness effect: 35 declines and five increases. Although highly unlikely,
221 using this criterion we therefore cannot rule out that all five fitness increases are false
222 positives.

223 **3.3. The *A. niger* fitness landscapes contain local maxima and minima**

224 If sign epistasis is locally consistent, it may lead to local fitness maxima surrounded
225 by genotypes of lower fitness, as well as to local fitness minima surrounded by genotypes
226 of higher fitness. We analyzed both data sets in order to detect local fitness maxima
227 and minima by comparing the fitness rank of all 32 genotypes with that of their five
228 single-mutation neighbors. This analysis shows several features that indicate the ruggedness
229 of these fitness landscapes (table 1, figure 2). First, the wild-type strain represents the
230 global maximum in both landscapes, but the quintuple mutant does not coincide with the
231 global minimum in either landscape; both data sets contain a genotype with lower fitness.
232 Second, in total four maxima and three minima are identified in CS I and three maxima and
233 two minima in CS II, emphasizing the ruggedness of these landscapes (see figure 2c and 2d).
234 To test whether these fitness maxima and minima differ from their mutational neighbors
235 (and are not part of a neutral fitness “plateau”), we performed one-sample one-tailed
236 t -tests with four degrees of freedom to test the fitness difference between the single mean
237 value of the focal genotype and that of its five neighbors. These showed that three of the
238 four maxima and two of the three minima of CS I are significant, while in CS II two of

239 the three maxima and both minima are significant (see table 1). Sequential-Bonferroni
240 correction (Rice 1989) leaves two maxima (the global and a local one) of CS I significant,
241 as well as the global maximum and global minimum (which is different from the quintuple
242 mutant) of CS II. Thus, while we are unable to identify individual cases of sign epistasis
243 with statistical confidence, these tests confirm the ruggedness of these landscapes caused by
244 sign epistasis leading to isolated fitness maxima and minima.

245 **3.4. Asexual adaptation on the *A. niger* landscapes is constrained**

246 Next, we consider the consequences of these empirical fitness landscapes for the problem
247 of the evolution of sex by exploring the constraints experienced by sexual and asexual
248 populations adapting on these landscapes. For this, we make two crucial assumptions. First,
249 we assume that adaptation happens by the transition (by mutation and/or recombination)
250 from one to another of the 32 genotypes, i.e. by substitutions of wild-type or mutant
251 alleles at the five loci only. Second, we assume that all fitness differences among strains are
252 real, and neglect the statistical issues involved in their significance. (If we would interpret
253 non-significant fitness differences as evidence for their neutrality, adaptive evolution on
254 these landscapes would hardly be possible, because not a single of the 120 possible pathways
255 involving the sequential substitution of five single mutations from quintuple mutant to wild
256 type would be accessible in either landscape.) Instead, we will deal with the (relative)
257 neutrality within these fitness landscapes by considering both sign and magnitude of the
258 fitness differences in our simulations.

259 We studied the adaptive dynamics of asexual populations for a wide range of parameter
260 values. In the strong selection-weak mutation (SSWM) limit ($NU \ln N \ll 1$ and $Ns \gg 1$
261 with s denoting a typical selection coefficient) where clonal interference (Gerrish and Lenski
262 1998; Park and Krug 2007) is unimportant, adaptation of an asexual population can be

263 approximated by an adaptive walk on the landscape. Here we will determine the probability
 264 that the adaptive walker will arrive at one of the local maxima when it starts from the
 265 quintuple mutant. To this end, we need to specify the probability that a walker located at
 266 a sequence σ jumps to one of its mutational neighbors, which reads (Orr 2002)

$$P(\sigma \rightarrow \sigma') = \frac{\pi(\sigma'; \sigma)}{\sum_{\sigma''} \pi(\sigma''; \sigma)}. \quad (5)$$

267 Here $\pi(\sigma'; \sigma)$ is the fixation probability of genotype σ' introduced as a single copy into
 268 a population of genotype σ , and the denominator sums these probabilities over the five
 269 nearest (i.e. with Hamming distance 1) neighbors of the genotype σ . In the context of
 270 the Wright-Fisher model, $\pi(\sigma'; \sigma)$ can be approximated as $\pi \approx 2s$ when the selection
 271 coefficient $s = w(\sigma')/w(\sigma) - 1$ is small and positive. We neglect the fixation probability of
 272 deleterious mutations. In the actual calculation we numerically solve the implicit equation
 273 $1 - \pi = \exp[-(1 + s)\pi]$ due to Haldane (1927), which is known to provide an accurate
 274 approximation for the exact fixation probability of the Wright-Fisher model (Barrett et al.
 275 2006). Then we enumerate all fitness increasing paths and assign a probability to each
 276 path using the transition probabilities from equation (5). Although the analysis is generally
 277 applicable to other initial conditions, we only give the results for the initial condition
 278 $\sigma = (11111)$.

279 The simulation results in the SSWM regime ($U = 10^{-8}$ and $N = 10^5$) on both
 280 landscapes are shown in figure 3 and table 2. Clearly, most adaptive walks end at a local
 281 maximum, and few reach the global maximum on both landscapes. The populations stay
 282 monomorphic most of the time alternated by brief periods of polymorphism during jumps to
 283 another peak. Mean fitness of 10,000 runs approaches asymptotic values of 0.90 and 0.94
 284 for CS I and CS II, respectively. These asymptotic values are consistent with predictions
 285 from the adaptive walk scenario.

286 Beyond the SSWM regime, there are two conspicuous regimes of asexual adaptation,
 287 which depend on the population size N and mutation rate U (Jain and Krug 2007).
 288 At very large N , the population behaves as in the infinite population limit and the
 289 evolutionary dynamics are completely deterministic. In this regime all possible genotypes
 290 are simultaneously present in the population (but most of them at extremely small
 291 frequencies). A simple algorithm exists to predict the trajectories of the most populated
 292 genotype that a population will follow from an arbitrary starting point to the global fitness
 293 maximum (Jain and Krug 2005; Jain 2007), see Appendix B. For our empirical landscapes
 294 these trajectories are:

$$11111 \rightarrow 11101 \rightarrow 00011 \rightarrow 00000 \quad \text{CS I}, \quad (6)$$

$$11111 \rightarrow 11110 \rightarrow 10110 \rightarrow 00000 \quad \text{CS II}. \quad (7)$$

295 Apart from the first step in (7), all intermediate genotypes appearing in these trajectories
 296 are local fitness maxima. We find that the deterministic regime is reached in our landscapes
 297 for population sizes exceeding $N \propto 1/U^2$ (see below).

298 Between the SSWM and the deterministic regime lies the locally deterministic regime
 299 of Jain and Krug (2007), where the population behaves deterministically up to a crossover
 300 time T_{\times} when the first local maximum is reached. This initial stage of adaptation can be
 301 described as a “greedy” adaptive walk that always chooses the nearest neighbor genotype of
 302 highest fitness and gets stuck at local maxima. For example, a greedy walker on landscape
 303 CS II starting from the sequence 11111 will take the steps $11111 \rightarrow 11110 \rightarrow 10110$ and
 304 on the CS I landscape the walk becomes $11111 \rightarrow 11101$. Beyond the initial stage the
 305 behavior is determined by the stochastic escape from local maxima by the creation of
 306 multiple mutants (Weinreich and Chao 2005). Provided the mutation rate is sufficiently
 307 small, the time scale for the escape dynamics is well separated from the greedy walk phase.

308 For larger populations the escape dynamics becomes deterministic as well, taking the form
309 of an “adaptive flight” between local maxima, as illustrated in (6) and (7).

310 In the following, the intermediate regime will be referred to as the ‘greedy walk’
311 regime. It sets in when the number NU of mutants produced in one generation exceeds the
312 number L of one-mutant neighbors of a given genotype. It should however be noted that
313 the boundaries between the different regimes are not sharply defined and may depend on
314 the details of the landscape (Jain and Krug 2007). The greedy walker concept allows us to
315 assign to each local maximum a basin of attraction that contains all genotypes that end up
316 at this maximum under the greedy walk dynamics. The basins of attraction for both fitness
317 landscapes are illustrated in color in the arrow plots of figure 2.

318 **3.5. Simulating the effect of sex on the *A. niger* landscape**

319 Given the adaptive constraints for asexuals, we ask whether sex and recombination can
320 be beneficial for adaptation on these landscapes. As a general first question, we ask whether
321 recombination among locally optimal genotypes is beneficial in the sense that it will either
322 create the globally most fit genotype (i.e. the wild-type), or a genotype that is part of the
323 basin of attraction of the global optimum. In CS I, three locally optimal genotypes exist,
324 but recombination among them cannot create the globally optimal wild-type (table 3).
325 Similarly, recombination between the two locally optimal genotypes of CS II does not create
326 the high-fitness wild-type. Rather, recombination has a direct negative effect on offspring
327 fitness on both landscapes. Although sex cannot generate the global optimum directly,
328 it can produce genotypes with access to the global optima via mutation and selection,
329 i.e. that appear in the basin of attraction of the global optimum (table 3). Thus, in a
330 polymorphic population with genotypes occupying local fitness maxima, recombination can
331 release populations that are stuck on local fitness peaks in both empirical landscapes and

332 allow them to evolve towards the global optimum. However, it is not clear which conditions
333 would lead to a polymorphic population occupying several fitness maxima.

334 In the following we therefore use simulations to ask whether and when sex provides
335 an adaptive advantage for a population that initially consists of the low-fitness quintuple
336 mutant on these landscapes. In the SSWM regime, the population remains monomorphic
337 most of the time, and only during the selective sweep there are two segregating sequences
338 (whose Hamming distance is 1 within our mutation scheme). Hence in this regime
339 recombination cannot play any role and the adaptive dynamics are the same for sexual and
340 asexual populations. For example, we simulated a sexual population with $r = 1$ and 0.01
341 using the same parameters as in figure 3, and we observed the same dynamics as for the
342 asexual population (data not shown).

343 *3.5.1. Infinite population size*

344 When the population size is large enough, the population can be polymorphic and
345 recombination may play a role. Let us first investigate the infinite population limit where
346 the dynamics are deterministic. The stochastic simulation can then be replaced by simply
347 iterating the mutation-selection recombination equation (4) with equations (1), (2) and
348 (3) for the population frequencies. Referring to the asexual trajectories (6) and (7), we
349 expect that the adaptive dynamics on the CS II landscape are simpler, in that only a single
350 intermediate fitness maximum is involved. We therefore begin with the analysis of CS II.

As figures 4 and 5 show, recombination on this landscape never confers an advantage,
rather sex is always deleterious. The disadvantage of sex is particularly dramatic for
 $r \geq 10^{-1}$, where recombination is seen to prevent the escape of the population from the
local maximum 10110. The suppression of the escape from a local fitness peak due to

recombination is well known from studies of two-locus models. In this context the notion of a *recombination barrier* was introduced, referring to the fact that the escape rate decreases exponentially with increasing recombination rate r (Stephan 1996; Weinreich and Chao 2005). Qualitatively the escape from the peak is suppressed by breaking up escape genotypes such as 10000, 00100 and 00010 which are at Hamming distance 2 from the local peak and at Hamming distance 1 from the wildtype, and which are destroyed by recombination with the (dominant) local peak genotype. For a rough estimate of this effect we may use the formula

$$r_{\text{crit}} \approx \frac{-s_{\text{ben}}}{1.27 + \ln(s_{\text{ben}})} \quad (8)$$

351 derived in (Weinreich and Chao 2005) within a two-locus model. Equation (8) expresses
 352 the critical recombination probability r_{crit} at which suppression of escape sets in as a
 353 function of the beneficial selection coefficient s_{ben} of the final peak relative to the initial
 354 peak. For the CS II landscape $s_{\text{ben}} \approx 0.06$, which yields $r_{\text{crit}} \approx 0.04$, in reasonable agreement
 355 with the numerically observed behavior. In the infinite population case, the escape time
 356 may actually diverge at a finite value of r , reflecting the appearance of a stationary
 357 mutation-selection-recombination equilibrium centered around the initial peak, in addition
 358 to the “true” equilibrium centered around the global optimum. Similar *bistable* behavior
 359 has been found in deterministic mutation-selection-recombination models with a single peak
 360 fitness landscape (Jacobi and Nordahl 2006).

361 The infinite population dynamics on landscape CS I are slightly more complicated.
 362 When $U \geq 10^{-1}$, recombination is always deleterious, because a recombinational load (as
 363 well as the mutation load) is observable, similar as for landscape CS II (fig. 4). However,
 364 when $U \leq 10^{-3}$, sex appears advantageous for some recombination rates, because the
 365 time to arrive at the globally optimal genotype is shorter than for the asexual population,
 366 although the time to escape from the local maximum (11101) is longer than for the asexual
 367 population (fig. 5). Closer inspection of this case reveals that recombination allows the

368 population to bypass the intermediate maximum 00011, but this mechanism is operative
 369 only in a narrow range (e.g., the range $0.08 \leq r \leq 0.12$ or $r \leq 0.03$ for $U = 10^{-5}$; data not
 370 shown). This implies that the escape time is a nonmonotonic function of r in this regime,
 371 with a well-tuned rate of recombination slightly accelerating the adaptation process; similar
 372 effects have been observed in two-locus simulations (Weinreich and Chao 2005). Note that
 373 local maximum 11101 is at the same mutational distance ($d = 4$) from both the intermediate
 374 maximum 00011 and the global maximum 00000. The reason for the detour performed by
 375 the asexual trajectory (6) is that 00011 is closer to the initial point 11111 than the global
 376 maximum (Jain and Krug 2005); indeed, an infinite asexual population starting from 11101
 377 moves directly to the global maximum, without visiting 00011 (data not shown).

378 3.5.2. *Finite population size*

379 For finite N , we simulated 10,000 independent runs for each parameter set. For
 380 $U = 10^{-1}$, the simulation results with $N = 10^3$ are already indistinguishable from the
 381 infinite population dynamics for both landscapes (fig. 4). We also simulated smaller
 382 population sizes ($N = 10, 100$) and observed qualitatively similar behavior (data not
 383 shown). We can therefore conclude that recombination is not advantageous on these
 384 empirical landscapes for any population size when the mutation rate is high.

385 The situation becomes slightly more complicated at intermediate population size for
 386 lower mutation rates. In the intermediate regime, where the dynamics are indistinguishable
 387 from a deterministic greedy walk up to the time at which a local maximum is reached
 388 (i.e., up to T_{\times}), sex is generally deleterious on landscape CS II. This is illustrated by the
 389 simulation results for $U = 10^{-3}$ and $N = 10^5$ in figure 6: there is a small advantage of
 390 recombination during the initial greedy walk stage where the dynamics are slightly different
 391 from deterministic dynamics, but during the final escape stage recombination is still

392 deleterious. We actually simulated a wider range of parameters (N up to 10^9 and U down
393 to 10^{-7}), but the qualitative behavior is more or less the same as in figure 6. Note, however,
394 that this slight advantage of sex during the early stages of adaptation is insignificant for
395 long-term adaptation, which is governed by the time needed to escape from a local peak.

396 As expected from the infinite population dynamics, landscape CS I shows more complex
397 adaptive behavior also for finite populations (fig. 7). Let us begin with the initial greedy
398 walk stage. Since the attractor of the quintuple mutant, i.e. the local maximum 11101, is
399 only one mutation away, we do not expect any difference between the asexual and the sexual
400 greedy walks. That is, up to the time when fitness reaches the value 0.858, one cannot see
401 any difference in the rate of adaptation between sexual and asexual populations. Hence, the
402 escape stage will be of main interest for landscape CS I. For large populations, adaptation
403 is governed by deterministic dynamics (see fig. 7a). It appears that the escape advantage
404 seen at intermediate r (fig. 7a) depends on a sufficiently large mutation supply rate: when
405 either N (fig. 7b) or U (fig. 7c) is lower, this benefit of recombination disappears. The fact
406 that we find the escape advantage of recombination on landscape CS I only, indicates that
407 it depends on the topographical details of the fitness landscape.

408 4. Discussion

409 While epistasis includes all possible forms of deviation from independent gene effects,
410 students of the evolution of sex have almost exclusively been interested in a single particular
411 form of magnitude epistasis, i.e. negative epistasis (Kondrashov 1993; Otto and Lenormand
412 2002; de Visser and Elena 2007; Kouyos et al. 2007). Negative epistasis is one possible
413 source of negative linkage disequilibrium and hence of a long-term advantage of sex
414 by increasing the genetic variation in fitness and accelerating adaptation; alternatively,
415 genetic drift combined with directional selection can cause negative linkage disequilibrium.

416 Despite increasing efforts to detect negative epistasis in recent years, the support for this
417 form of epistasis is weak (de Visser and Elena 2007; Kouyos et al. 2007). However, other
418 forms of epistasis may be relevant for the problem of the evolution of sex as well. For
419 instance, sign epistasis, causing variation in the sign of the fitness effect of mutations across
420 genotypes, may impose adaptive constraints caused by valleys of low fitness separating
421 fitness maxima (Weinreich et al. 2005; Weinreich and Chao 2005). Whether and when
422 recombination may facilitate adaptation on such rugged fitness landscapes is largely
423 unknown and depends in part on the topography of the fitness landscape (i.e. the number,
424 height and distance of fitness peaks).

425 In the present study, we have analyzed fitness data from two sets of 32 strains of
426 the fungus *A. niger* carrying all possible combinations of five mutations with individually
427 deleterious effect. In a previous study (de Visser et al. 1997), we used these strains to detect
428 magnitude epistasis by studying the overall relationship between mean fitness and mutation
429 number. We found no support for prevailing negative or positive epistasis, despite significant
430 magnitude epistasis of both signs for particular pairs of mutations. Our new analyses were
431 aimed at detecting sign epistasis and describing the fitness landscapes for these sets of five
432 loci. We found that among the 128 unique single-mutation steps present in the two sets
433 combined, 38 cause fitness increases, despite their individually deleterious effect in the wild
434 type. In addition, when we compared the fitness of each strain with its five single-mutation
435 neighbors, we found several fitness maxima and minima in both sets of strains, nine of
436 which are statistically significant (four after correcting for multiple comparisons). These
437 fitness maxima and minima indicate ruggedness of the fitness landscapes resulting from
438 sign epistasis.

439 We then used simulations with the Wright-Fisher model to study whether and when
440 recombination might facilitate adaptation on these empirical fitness landscapes. We first

441 found that adaptation was constrained for asexual populations, as only a minority of
442 adaptive walks of finite populations from the low-fitness quintuple mutants ended at
443 the global fitness optimum (see fig. 3), and even infinitely large populations adapt by
444 sequentially visiting local maxima [equations (6) and (7)]. The simulations showed that
445 adaptation on these rugged landscapes generally involved two distinct stages: the approach
446 to local optimum and the escape from a local optimum to a new optimum.

447 Two general conclusions can be drawn from the simulations comparing asexual and
448 sexual populations. First, recombination provides a small benefit during the approach to a
449 local optimum at intermediate N and U , if the local optimum is more than one mutation
450 removed from the ancestral genotype. This small benefit is probably due to the fact that
451 the alleles involved in the local optimal genotype are in negative linkage disequilibrium due
452 to drift and selection, causing recombination to combine them more often than to disrupt
453 them (Fisher 1930; Muller 1932). This effect becomes more pronounced as the distance to
454 the global peak increases. We have verified in simulations that recombination results in a
455 significant speedup of adaptation in a five-locus system without epistatic interactions (data
456 not shown; see Kondrashov and Kondrashov (2001) and Kim and Orr (2005) for similar
457 results). However, this small advantage is generally insignificant for long-term adaptation,
458 which is limited by the time needed to escape from a local peak.

459 Second, during the escape stage the effect of recombination is generally deleterious and
460 increases the time to escape from the local optimum. At high recombination rates ($r = 1$),
461 we only observed deleterious effects, which are caused by the net break down of escape
462 genotypes once they arise by mutation (Stephan 1996; Weinreich and Chao 2005). We also
463 found some conditions where sex and recombination could facilitate the population's escape.
464 The fact that we only observed benefits of recombination for one landscape indicates that
465 the landscape's specific topography is involved in this benefit. Also, the escape benefit

466 is only apparent when N and U are sufficiently high (see fig. 7), consistent with the
467 dependence of any advantage of recombination on a sufficiently polymorphic population.
468 In a more general sense, the effect of recombination during the escape stage will depend
469 on conditions where the alleles necessary for the escape genotype are present in negative
470 linkage disequilibrium in genotypes with relatively high fitness.

471 Few theoretical studies have considered the effect of sex and recombination on rugged
472 fitness landscapes. Kondrashov and Kondrashov (2001) found a general disadvantage of sex
473 in a particular two-dimensional landscape with a single ‘smooth’ ridge towards high fitness
474 and no local fitness maxima. Later, Watson and Wakeley (2006) modified this landscape
475 and found conditions where sex does provide an advantage. The landscapes considered in
476 these papers are similar to ours in that most paths to the global optimum are inaccessible
477 to adaptive evolution, but they differ in that they contain extended neutral networks
478 instead of local fitness peaks. On the other hand, Hadany and Beker (2003) found a general
479 advantage of recombination in simulations of rather small populations in fitness landscapes
480 generated according to Kauffman’s NK-model (Kauffman 1993). Together with the work
481 presented here, these fragmentary results suggest that the effects of recombination depend
482 on features of the landscape topography which go beyond the mere presence or absence of
483 sign epistasis. The precise nature of these features remains to be elucidated in future work.

484 How do we reconcile our finding of a general lack of sex benefit on rugged fitness
485 landscapes with the several experimental reports of faster evolving sexual compared to
486 asexual populations (e.g. Rice (2002); de Visser and Elena (2007))? The reports of sex
487 benefits suggest that the fitness landscapes involved have different topographies from ours,
488 e.g. contain smooth areas or ridges allowing unconstrained adaptation. These differences
489 could have a variety of causes. First, our landscapes are based on the interactions
490 among mutations with individually deleterious effect, which may differ systematically

491 from those involving beneficial mutations. A similar study of the fitness landscape of
492 TEM-1 β -lactamase involving five mutations with jointly beneficial effects also found sign
493 epistasis and local ruggedness (Weinreich et al. 2006), but did not find the severe adaptive
494 constraints imposed by isolated local fitness maxima that we found. We are unaware of
495 other data sets that would allow a more systematic test whether the nature of the mutations
496 studied is responsible for the differences in landscape topographies. Second, sampling error
497 from studying only a handful of loci may cause our landscape to ‘miss’ smooth ridges or
498 surfaces connecting local peaks, particularly if those are rare. Third, the topography of
499 fitness landscapes may depend on the level of fitness. A study of protein fitness landscapes
500 found a relative smooth surface for low-fitness proteins, and ruggedness above a certain
501 fitness value (Hayashi et al. 2006). If ruggedness appears to be a typical feature of regions
502 of relatively high fitness, our results suggest that sex would be beneficial only for low-fitness
503 individuals, consistent with the negative correlation between fitness and recombination
504 rates observed for many organisms (Hadany and Beker 2003).

505 Schoustra et al. (2007) recently observed a specific advantage for mitotic recombination
506 in the face of sign epistasis in the homothallic fungus *Aspergillus nidulans*. By comparing
507 adaptation in diploid and haploid strains, they found that four diploid strains that
508 spontaneously reverted to haploidy gained the highest fitness. Back-crosses of these lines
509 showed that multiple mutations were present, some of which had individually deleterious
510 effect. Therefore, these lines seemed to have accumulated recessive deleterious mutations
511 when diploid, which showed their combined beneficial effect in haploid recombinants
512 produced in the parasexual cycle. The advantage of recombination in rugged fitness
513 landscapes may thus depend on the relative length of the diploid and haploid phase of the
514 sexual cycle, which affect the adaptive constraints experienced from fitness valleys.

515 In conclusion, further progress in our understanding of the costs and benefits of

516 recombination will increasingly depend on the combination of experimental studies of the
 517 structure of real fitness landscapes with population-genetic simulations comparing different
 518 reproductive strategies. In the present paper we have attempted a modest first step in this
 519 direction.

520 We thank Rolf Hoekstra, Duur Aanen, Fons Debets, Yuseob Kim and Alexander Klözer
 521 for valuable discussion and/or comments on the manuscript. This work has been supported
 522 by DFG within SFB 680 *Molecular Basis of Evolutionary Innovations*.

523 A. Other recombination schemes

524 In this appendix, we describe how two other recombination schemes (one site exchange
 525 and single crossover) are implemented.

526 One site exchange means that two genotypes may exchange only one locus. Using the
 527 same exemplar sequences as in the main text (11101 and 10100), the outcome would be
 528 11101, 10100, 10101, and 11100. Unlike free recombination, the probability of having one of
 529 the above outcomes is different; in this example, 11101 and 10100 can occur with conditional
 530 probability $\frac{3}{10}$ and 10101 and 11100 can occur with probability $\frac{1}{5}$ under the condition that
 531 recombination happens. The explicit form of $W_{\sigma|\sigma'\sigma''}$ for the one site exchange rule is

$$W_{\sigma|\sigma'\sigma''} = (1 - \delta_{\sigma'\sigma''}) \left[(\delta_{\sigma\sigma'} + \delta_{\sigma\sigma''}) \frac{1}{2} + \frac{rd(\sigma', \sigma'')}{2L} + (1 - \delta_{\sigma\sigma'}) (1 - \delta_{\sigma\sigma''}) Z_{\sigma|\sigma'\sigma''} \frac{r}{2L} \right] + \delta_{\sigma\sigma'} \delta_{\sigma\sigma''} \quad (\text{A1})$$

532 where

$$Z_{\sigma|\sigma'\sigma''} = \begin{cases} 2 & \text{if } d(\sigma', \sigma'') = 2 \text{ and } d(\sigma, \sigma') = d(\sigma, \sigma'') = 1, \\ 1 & \text{if } d(\sigma', \sigma'') > 2 \text{ and } d(\sigma, \sigma') = 1, \ d(\sigma, \sigma'') = d(\sigma', \sigma'') - 1, \\ 1 & \text{if } d(\sigma', \sigma'') > 2 \text{ and } d(\sigma, \sigma'') = 1, \ d(\sigma, \sigma') = d(\sigma', \sigma'') - 1, \\ 0 & \text{otherwise.} \end{cases}$$

533 A crossover divides each genotype into two parts at the same randomly chosen position
 534 between two loci and mixes them to form new genotypes. If, say, crossover happens between
 535 the two parents of our example (11101 and 10100), the resulting pair would be either 11100
 536 and 10100 (with probability $\frac{1}{4}$), or 10101 and 11101 (with probability $\frac{3}{4}$). As before, only
 537 one of the pair will join the next generation. For the crossover, $W_{\sigma|\sigma'\sigma''}$ takes the form

$$W_{\sigma|\sigma'\sigma''} = (1 - \delta_{\sigma'\sigma''}) \left[(\delta_{\sigma\sigma'} + \delta_{\sigma\sigma''}) \left(\frac{1}{2} - \frac{\ell_d - \ell_1}{2(L-1)} r \right) + (1 - \delta_{\sigma\sigma'}) (1 - \delta_{\sigma\sigma''}) C_{\sigma|\sigma'\sigma''} \frac{r}{2(L-1)} \right] + \delta_{\sigma\sigma'} \delta_{\sigma\sigma''}, \quad (\text{A2})$$

538 where d (although we omit the arguments) is the Hamming distance between σ' and σ'' , ℓ_i
 539 ($i = 1, \dots, d$) stands for the location of the i^{th} different locus between σ' and σ'' counted
 540 from the left, and $C_{\sigma|\sigma'\sigma''} = \ell_{j+1} - \ell_j$ if the crossover occurring between loci ℓ_{j+1} and ℓ_j
 541 ($j = 1, \dots, d - 1$) can result in a genotype σ and 0 otherwise.

542 B. Adaptive flight trajectories

543 Here we briefly outline the procedure that leads to the adaptive trajectories (6)
 544 and (7) for the most populated genotype in the infinite population case; for details see
 545 (Krug and Karl 2003; Jain and Krug 2005; Jain 2007). The key idea is to subdivide the
 546 genotype space into *shells* of equal Hamming distance from the initial genotype, which
 547 in our case is the quintuple mutant 11111. Because all genotypes in a shell are fed by

548 mutations at the same rate, only the most fit genotype in a shell has a chance to reach a
549 significant frequency in the infinite population limit. The largest fitness value within a shell
550 defines the *shell fitness*. Moreover, as the population supply by mutations from the initial
551 genotype decreases exponentially with increasing Hamming distance, distant shells can
552 become highly populated only if the corresponding shell fitness is larger than the fitnesses
553 of all shells that are closer to the initial genotype. In short, the adaptive trajectory can
554 only contain genotypes that are *records* in the sequence of shell fitnesses.

555 As an example, consider the CSI landscape. The fittest genotypes in the different shells
556 are 11101 ($d = 1$), 11001 ($d = 2$), 00011 ($d = 3$), 10000 ($d = 4$) and 00000 ($d = 5$). As the
557 fitness of 11001 is lower than that of 11101, and the fitness of 10000 is lower than that of
558 00011, the sequence of record genotypes is $11111 \rightarrow 11101 \rightarrow 00011 \rightarrow 00000$. In general,
559 some of the record genotypes may disappear from the trajectory because they are *bypassed*
560 by genotypes of higher fitness that are located further away from the initial genotype, but
561 for the landscapes CSI and CSII this does not occur. A careful analysis of the deterministic
562 mutation-selection equations shows that this procedure becomes exact in the limit $U \rightarrow 0$
563 (Jain 2007).

REFERENCES

564

565 Barrett, R. D. H., K. M’Gonigle, and S. P. Otto. 2006. The distribution of beneficial mutant
566 effects under strong selection. *Genetics* 174:2071–2079.

567 Barton, N. H. 1995. A general model for the evolution of recombination. *Genetical Research*
568 65:123-144.

569 Buckling, A., M. A. Wills, and N. Colegrave. 2003. Adaptation limits diversification of
570 experimental bacterial populations. *Science* 302:2107–2109.

571 Burch, C. L., and L. Chao. 2000. Evolvability of an RNA virus is determined by its
572 mutational neighbourhood. *Nature* 406:625–628.

573 de Visser, J. A. G. M., and S. F. Elena. 2007. The evolution of sex: empirical insights into
574 the roles of epistasis and drift. *Nature Reviews Genetics* 8:139–149.

575 de Visser, J. A. G. M., R. F. Hoekstra, and H. van den Ende. 1997. Test of interaction
576 between genetic markers that affect fitness in *Aspergillus niger*. *Evolution*
577 51:1499–1505.

578 Fisher, R. A. 1930. *The Genetical Theory of Natural Selection*. Clarendon Press, Oxford.

579 Gerrish, P. J., and R. E. Lenski. 1998. The fate of competing beneficial mutations in an
580 asexual population. *Genetica* 102/103: 127–144.

581 Hadany, L., and T. Beker. 2003. Fitness-associated recombination on rugged adaptive
582 landscapes. *Journal of Evolutionary Biology* 16:862–870.

583 Haldane, J. B. S. 1927. The mathematical theory of natural and artificial selection, part
584 V: selection and mutation. *Proceedings of the Cambridge Philosophical Society*
585 23:838–844.

- 586 Hayashi, Y., T. Aita, H. Toyota, Y. Husimi, I. Urabe, and T. Yomo. 2006. Experimental
587 rugged fitness landscape in protein sequence space. *PLoS One* 1:e96
- 588 Jacobi, M. N., and M. Nordahl. 2006. Quasispecies and recombination. *Theoretical*
589 *Population Biology* 70:479–485.
- 590 Jain, K. 2007. Evolutionary dynamics of the most populated genotype on rugged fitness
591 landscapes. *Physical Review E* 76:031922.
- 592 Jain, K., and J. Krug. 2005. Evolutionary trajectories in rugged fitness landscapes. *Journal*
593 *of Statistical Mechanics: Theory and Experiment* P04008.
- 594 Jain, K., and J. Krug. 2007. Deterministic and stochastic regimes of asexual evolution on
595 rugged fitness landscapes. *Genetics* 175:1275–1288.
- 596 Kauffman, S. A. 1993 *The Origins of Order. Self-Organization and Selection in Evolution.*
597 Oxford University Press, Oxford.
- 598 Kim, Y., and H.A. Orr. 2005. Adaptation in Sexuals vs. Asexuals: Clonal Interference and
599 the Fisher-Muller Model. *Genetics* 171:1377–1386.
- 600 Krug, J., and C. Karl. 2003. Punctuated evolution for the quasispecies model. *Physica A*
601 318:137–143.
- 602 Kondrashov, A. S. 1993. Classification of hypotheses on the advantage of amphimixis.
603 *Journal of Heredity* 84:372–387.
- 604 Kondrashov, F. A., and A. S. Kondrashov. 2001. Multidimensional epistasis and the
605 disadvantage of sex. *Proceedings of the National Academy of Sciences USA*
606 98:12089–12092.

- 607 Korona, R., C. H. Nakatsu, L. J. Forney, and R. E. Lenski. 1994. Evidence for multiple
608 adaptive peaks from populations of bacteria evolving in a structured habitat.
609 *Proceedings of the National Academy of Sciences USA* 91:9037–9041.
- 610 Kouyos, R. D., O. K. Silander, and S. Bonhoeffer. 2007. Epistasis between deleterious
611 mutations and the evolution of recombination. *Trends in Ecology and Evolution*
612 22:308–315.
- 613 Muller, H. J. 1932. Some genetic aspects of sex. *American Naturalist* 66:118–138.
- 614 Orr, H. A. 2002. The population genetics of adaptation: the adaptation of DNA sequences.
615 *Evolution* 56:1317–1330.
- 616 Otto, S. P., and T. Lenormand. 2002. Resolving the paradox of sex and recombination.
617 *Nature Review Genetics* 3:252–261.
- 618 Park, S.-C., and J. Krug. 2007. Clonal interference in large populations, *Proceedings of the*
619 *National Academy of Science USA* 104:10835–10840.
- 620 Poelwijk, F. J., D. J. Kiviet, D. M. Weinreich, and S. J. Tans. 2007. Empirical fitness
621 landscapes reveal accessible evolutionary paths. *Nature* 445:383–386.
- 622 Pringle, A., and J. W. Taylor. 2002. The fitness of filamentous fungi. *Trends in Microbiology*
623 10:474–481.
- 624 Rice, W. R. 1989. Analyzing tables of statistical tests. *Evolution* 43:223–225.
- 625 ——. 2002. Experimental tests of the adaptive significance of sexual recombination. *Nature*
626 *Review Genetics* 3:241–251.
- 627 Rozen, D. E., M. G. J. L. Habets, A. Handel, and J. A. G. M. De Visser. 2008. Heterogeneous
628 adaptive trajectories of small populations on complex fitness landscapes. *PLoS One*
629 3:e1715.

- 630 Schoustra, S. E., A. J. M. Debets, M. Slakhorst, and R. F. Hoekstra. 2007. Mitotic
631 recombination accelerates adaptation in the fungus *Aspergillus nidulans*. PLoS
632 Genetics 3:e68.
- 633 Stephan, W. 1996. The rate of compensatory evolution. Genetics 144:419–426.
- 634 Watson, R. A., and J. Wakeley. 2006. Multidimensional epistasis and the advantage of sex.
635 Proceedings of the 2005 Congress on Evolutionary Computation (CEC 2005).
- 636 Weinreich, D. M., and L. Chao. 2005. Rapid evolutionary escape by large populations from
637 local fitness peaks is likely in nature. Evolution 59:1175–1182.
- 638 Weinreich, D. M., N. F. Delaney, M. A. DePristo, and D. L. Hartl. 2006. Darwinian
639 evolution can follow only very few mutational paths to fitter proteins. Science
640 312:111–114.
- 641 Weinreich, D. M., R. A. Watson, and L. Chao. 2005. Perspective: Sign epistasis and genetic
642 constraint on evolutionary trajectories. Evolution 59:1165–1174.
- 643 Wolf, J. B., E. D. Brodie, and M. J. Wade. 2000. Epistasis and the evolutionary process.
644 Oxford, Oxford University press.
- 645 Wright, S. 1931. Evolution in Mendelian populations. Genetics 16:97–159.

Table 1. Analysis of local and global fitness maxima and minima on both *A. niger* landscapes.

Strain	Genotype ¹	Neighbors ²	CS I			CS II		
			w	Rank	Max/Min ³	w	Rank	Max/Min ³
1	00000	2,3,4,5,6	1	1	<u>Max</u> ^{***}	1	1	<u>Max</u> ^{**}
2	10000	1,7,8,9,10	0.878	3		0.878	6	
3	01000	1,7,11,12,13	0.835	10		0.835	13	
4	00100	1,8,11,14,15	0.870	5		0.870	7	
5	00010	1,9,12,14,16	0.772	20		0.909	4	
6	00001	1,10,13,15,16	0.793	16	Min*	0.772	21	
7	11000	2,3,17,18,19	0.865	6		0.865	8	
8	10100	2,4,17,20,21	0.854	8		0.854	11	
9	10010	2,5,18,20,22	0.773	19		0.923	3	
10	10001	2,6,19,21,22	0.873	4		0.773	20	
11	01100	3,4,17,23,24	0.816	14		0.816	16	
12	01010	3,5,18,23,25	0.716	24		0.852	12	
13	01001	3,6,19,24,25	0.848	9	Max	0.716	26	
14	00110	4,5,20,23,26	0.778	18		0.855	10	
15	00101	4,6,21,24,26	0.820	12		0.778	19	
16	00011	5,6,22,25,26	0.972	2	Max ^{***}	0.785	18	
17	11100	7,8,11,27,28	0.816	13		0.816	15	
18	11010	7,9,12,27,29	0.748	23		0.879	5	
19	11001	7,10,13,28,29	0.832	11		0.748	23	
20	10110	8,9,14,27,30	0.749	22		0.942	2	Max*

Table 1—Continued

Strain	Genotype ¹	Neighbors ²	CS I			CS II		
			w	Rank	Max/Min ³	w	Rank	Max/Min ³
21	10101	8,10,15,28,30	0.792	17		0.749	22	
22	10011	9,10,16,29,30	0.753	21		0.795	17	
23	01110	11,12,14,27,31	0.617	32	<u>Min</u> *	0.858	9	Max
24	01101	11,13,15,28,31	0.810	15		0.617	32	<u>Min</u> *
25	01011	12,13,16,29,31	0.643	31	Min	0.724	25	
26	00111	14,15,16,30,31	0.671	27		0.745	24	
27	11110	17,18,20,23,32	0.690	26		0.825	14	
28	11101	17,19,21,24,32	0.855	7	Max*	0.690	27	
29	11011	18,19,22,25,32	0.649	28		0.665	29	
30	10111	20,21,22,26,32	0.692	25		0.686	28	
31	01111	23,24,25,26,32	0.643	30		0.640	30	
32	11111	27,28,29,30,31	0.645	29		0.622	31	Min*

¹Zero and 1 indicate the absence or presence of a mutation in chromosomal order: *arg*, *pyr*, *leu*, *oli* and *crn* for the CS I landscape, and *arg*, *pyr*, *leu*, *phe* and *oli* for the CS II landscape.

²Neighbors are genotypes (strain numbers) that differ at a single locus.

³“Max” and “Min” indicate the presence of local fitness maxima or minima, with the global maximum and minimum of each landscape underlined; significant fitness maxima and minima

tested with 1-sample 1-tailed t -tests after sequential-Bonferroni correction indicated in bold face; * = $P < 0.05$, ** = $P < 0.01$, and *** = $P < 0.001$.

Table 2. Summary of the adaptive walks on both landscapes.

CS I		CS II	
Maximum	Adaptive walk weight ¹	Maximum	Adaptive walk weight ¹
00000	0.294	00000	0.134
00011	0.033	10110	0.757
11101	0.672	01110	0.109
01001	0.001		

¹Shown are the probabilities that the adaptive walker which starts at the sequence 11111 will visit one of the fitness maxima that are present (see table 1). The wild-type genotype (00000) represents the global maximum in both landscapes, the other are local maxima.

Table 3. Recombination among locally optimal genotypes on both *A. niger* adaptive landscapes.

Parents	Offspring ¹	Effect on mean fitness ²
CS I		
1. 01001 x 00011	<u>00001</u> , 01001, 00011, 01011	-0.096
2. 01001 x 11101	01001, <u>11001</u> , 01101, 11101	-0.015
3. 00011 x 11101	<u>00001</u> , <u>10001</u> , 01001, <u>00101</u> , 00011, <u>11001</u> , <u>10101</u> , 10011, 01101, 01011, 00111, 11101, <u>11011</u> , <u>10111</u> , 01111, 11111	-0.145***
CS II		
1. 10110 x 01110	00110, 10110, 01110, 11110	-0.030

¹Genotypes that are part of the basin of attraction of the globally optimal wild-type are underlined (shown in black in fig. 2a and 2b).

²Mean offspring fitness – mean parental fitness, tested with 1-sample 2-tailed *t*-test; *** : $P < 0.001$.

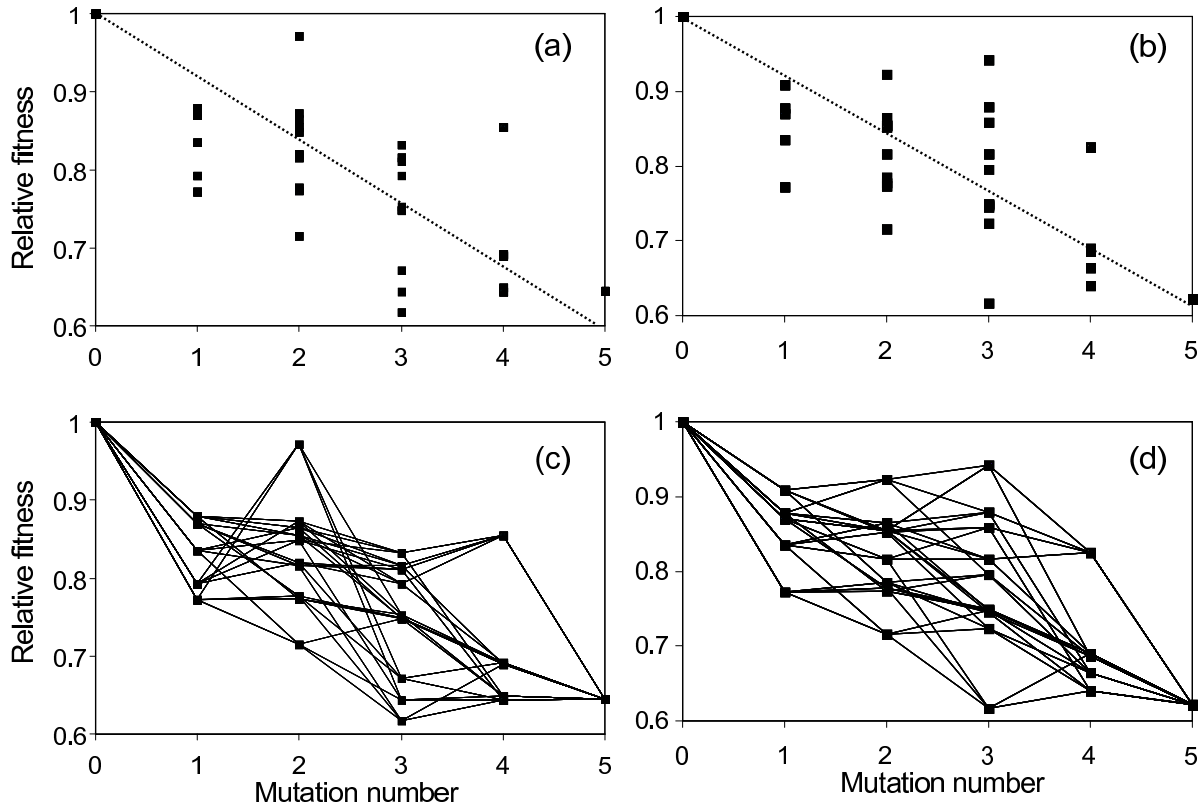


Fig. 1.— Relative fitness versus mutation number for both complete subsets (CS) of 32 strains of *A. niger*; these include *arg*, *pyr*, *leu*, *oli* and *crn* for CS I, and *arg*, *pyr*, *leu*, *phe* and *oli* for CS II. The overall relationship between fitness and mutation number is best described by a linear model (dashed line), both for CS I (a) and CS II (b). A model including a quadratic term does not improve the fit significantly (see text), suggesting the absence of a prevailing form of magnitude epistasis. When the 120 possible (direct, i.e. involving five mutations) pathways between wild-type and quintuple mutant are considered, mutations have negative or positive effect, depending on the genetic background, both for CS I (c) and CS II (d), indicating sign epistasis. The lines connect genotypes that differ at a single locus (i.e. Hamming distance = 1).

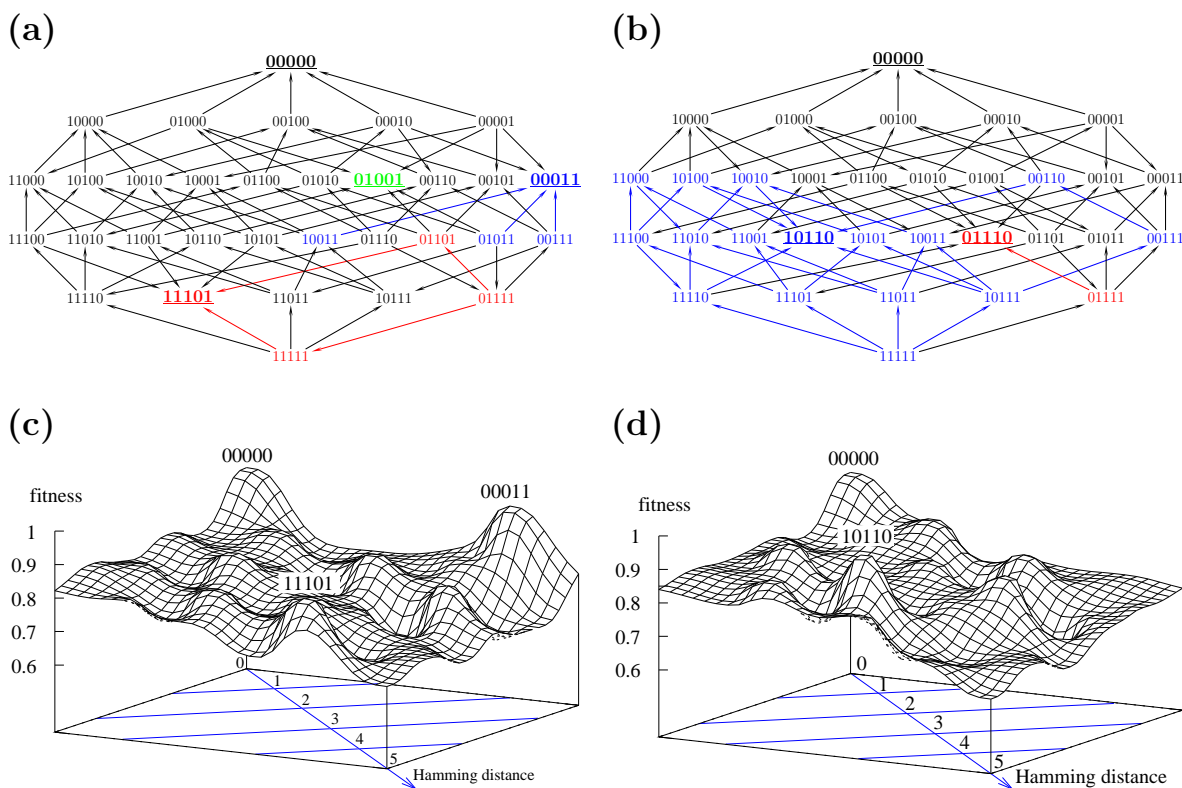


Fig. 2.— Fitness landscapes for both data sets. (a) Arrow plot for CS I. Arrows indicate single-mutation steps directed towards the genotype with higher fitness. Genotypes corresponding to fitness maxima are shown in larger font size and underlined. Different colors indicate which genotypes are in the basin of attraction of the various fitness maxima; genotype 01001 shown in green has only itself as basin of attraction. (b) Arrow plot for CS II. (c) Rendering of the CS I fitness landscape as a two-dimensional surface. The genotypes were arranged in a diamond-shaped area which mimicks the arrangement in the arrow plots in parts (a) and (b), and the fitness values of the genotypes were interpolated by a smooth function. The most prominent fitness maxima are highlighted, and the lines in the base plane indicate the positions of genotypes with equal numbers of mutations. (d) Two-dimensional surface plot for CSII.

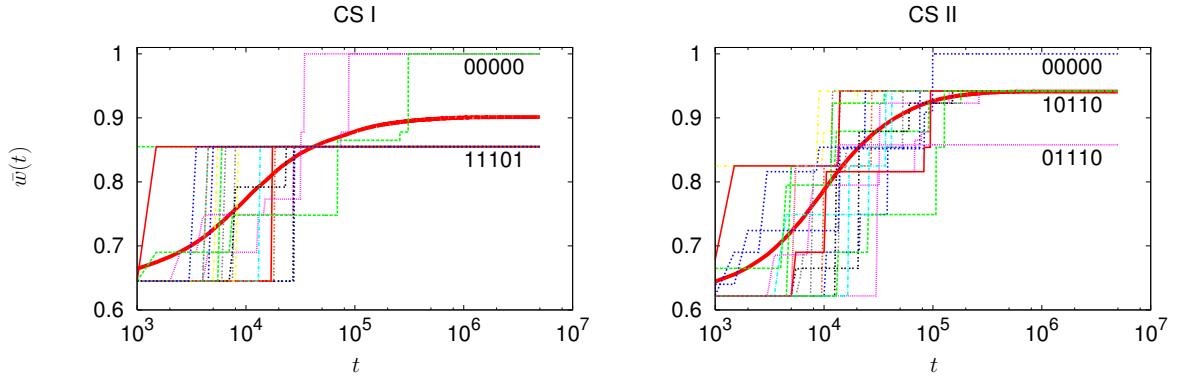


Fig. 3.— 20 sample adaptive walks starting with genotype 11111 on two empirical landscapes in the SSWM regime ($N = 10^5$ and $U = 10^{-8}$). On the CS I landscape, 17 adaptive walkers arrive at local maximum 11101 and only three walkers could reach the global maximum. The probability to arrive at two other local optima (01001 and 00011) is so low that no walker among 20 samples could reach them (see table 2). On the CS II landscape, 18 adaptive walks reached local maximum 10110 and only one walker could reach 00000 or the other local maximum 01110. The smooth thick red curves are the average of 10,000 independent adaptive walks.

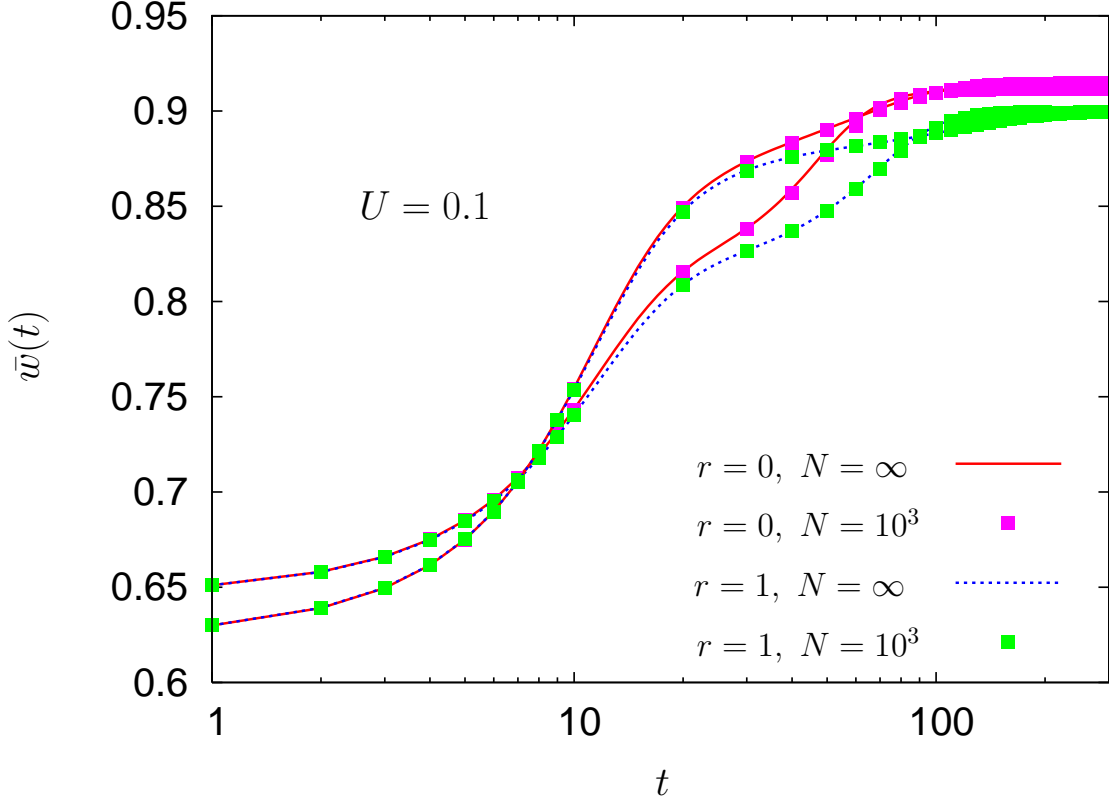


Fig. 4.— The effect of sex during adaptation on empirical fitness landscapes for high mutation rates ($U = 10^{-1}$). Shown are semi-logarithmic plots of mean fitness as a function of time (in generations) for 10,000 independent runs with ($r = 1$) or without ($r = 0$) recombination. Simulation results for finite ($N = 10^3$, symbols) and infinite population size (lines) are indistinguishable. The data sets starting at fitness 0.65 are results for the CS I landscape, those starting at lower fitness are for the CS II landscape. The mutational load (i.e. the difference between final asexual fitness and 1) and the recombinational load (i.e. the difference between fitness of the sexual and asexual populations) do not strongly depend on the particular landscape.

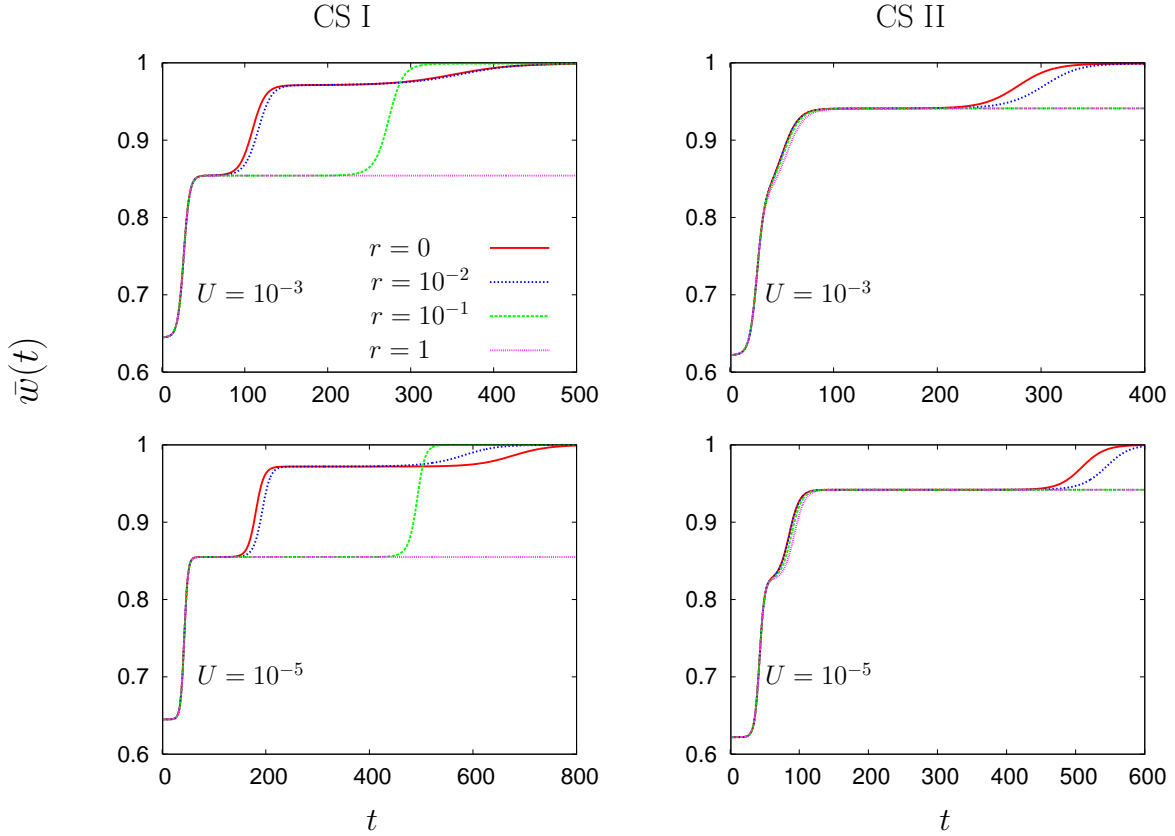


Fig. 5.— Infinite population dynamics during adaptation on two empirical fitness landscapes, CS I (left) and CS II (right), with and without recombination and $U < 10^{-1}$. For CS I, sex is initially deleterious, but low rates of recombination (r) later become advantageous during the escape from the first local optimum (genotype 11101 with fitness 0.855), where the second optimum (00011 with fitness 0.972) is bypassed when $r = 10^{-1}$. For CS II, recombination is always disadvantageous.

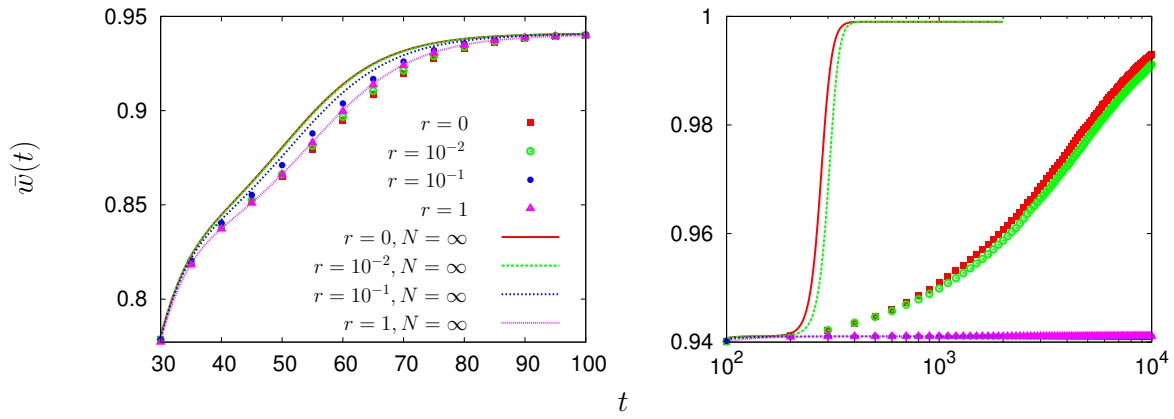


Fig. 6.— Adaptive dynamics during the greedy walk to (left panel), and escape from (right panel), the local optimum for CS II (genotype 10110 with fitness 0.942). Shown are the trajectories of mean fitness of 10^4 independent runs for $U = 10^{-3}$ and $N = 10^5$. The dynamics deviate from the deterministic dynamics, and recombination is slightly advantageous during the greedy walk regime, but still disadvantageous during the escape from the local optimum.

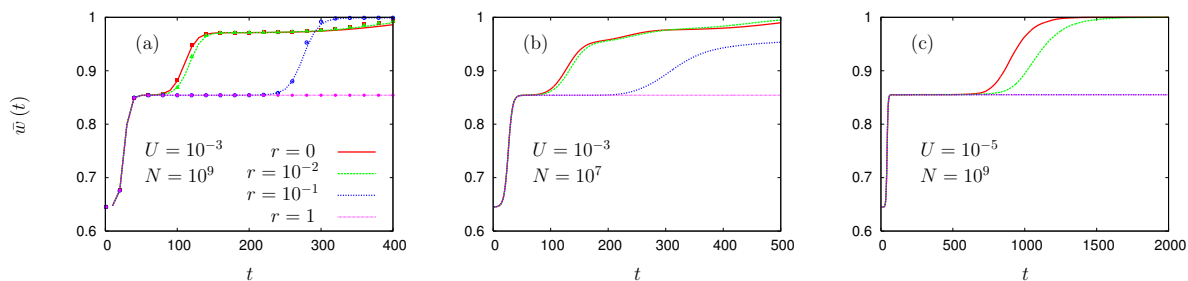


Fig. 7.— Adaptive dynamics for CS I for three different parameter sets (mean fitness trajectories of 10,000 independent runs). (a) The adaptive dynamics of the finite populations (symbols) resemble the deterministic behavior (lines). For $r = 10^{-1}$, the population bypasses the second local optimum (00011 with fitness 0.972). Bypassing due to recombination does not happen when either N (b) or U (c) are lower, although there is a slight advantage of sex in the escape stage for $r = 10^{-2}$ for the conditions of panel (b); the lines in panels (b) and (c) show the finite population results.